Dissociation of antibacterial activity and aminoglycoside ototoxicity in the 4-monosubstituted 2-deoxystreptamine apramycin

Tanja Matt[a,1], Chyan Leong Ng[b,1,2], Kathrin Lang[b,1], Su-Hua Sha[c,1,3], Rashid Akbergenov[a,1], Dmitri Shcherbakov[a,1], Martin Meyer[a], Stefan Duscha[a], Jing Xie[c,4], Srinivas R. Dubbaka[d], Déborah Perez-Fernandez[d], Andrea Vasella[d], V. Ramakrishnan[b], Jochen Schacht[c], and Erik C. Böttger[a,5]

[a]Institut für Medizinische Mikrobiologie, Universität Zürich, 8006 Zürich, Switzerland; [b]Structural Studies Division, Medical Research Council (MRC) Laboratory of Molecular Biology, Cambridge CB2 0QH, United Kingdom; [c]Kresge Hearing Research Institute, Department of Otolaryngology, Head and Neck Surgery, University of Michigan, Ann Arbor, MI 48109; and [d]Laboratorium für Organische Chemie, Eidgenössische Technische Hochschule Zürich, 8093 Zürich, Switzerland

Edited* by Gottfried Schatz, University of Basel, Reinach, Switzerland, and approved May 14, 2012 (received for review March 13, 2012)

Aminoglycosides are potent antibacterials, but therapy is compromised by substantial toxicity causing, in particular, irreversible hearing loss. Aminoglycoside ototoxicity occurs both in a sporadic dose-dependent and in a genetically predisposed fashion. We recently have developed a mechanistic concept that postulates a key role for the mitochondrial ribosome (mitoribosome) in aminoglycoside ototoxicity. We now report on the surprising finding that apramycin, a structurally unique aminoglycoside licensed for veterinary use, shows little activity toward eukaryotic ribosomes, including hybrid ribosomes which were genetically engineered to carry the mitoribosomal aminoglycoside-susceptibility A1555G allele. In ex vivo cultures of cochlear explants and in the in vivo guinea pig model of chronic ototoxicity, apramycin causes only little hair cell damage and hearing loss but it is a potent antibacterial with good activity against a range of clinical pathogens, including multidrug-resistant *Mycobacterium tuberculosis*. These data provide proof of concept that antibacterial activity can be dissected from aminoglycoside ototoxicity. Together with 3D structures of apramycin-ribosome complexes at 3.5-Å resolution, our results provide a conceptual framework for further development of less toxic aminoglycosides by hypothesis-driven chemical synthesis.

antibiotic | translation | misreading | deafness | mycobacteria

Aminoglycosides form a large family of water-soluble, polycationic amino sugars that are used as broad-spectrum antibacterial agents (1, 2). Aminoglycosides target the ribosome by direct interaction with ribosomal RNA (3), and they affect protein synthesis by inducing codon misreading and by inhibiting translocation of the tRNA–mRNA complex (4–9). Their binding site is within a conserved loop of 16S rRNA helix 44, which is part of the small ribosomal subunit's aminoacyl-tRNA acceptor site (A-site) (3, 10–12). Mutagenesis studies have dissected the contribution of individual rRNA nucleotides to drug–ribosome interaction (13). The selective activity of these compounds (i.e., their preferential binding to the bacterial as opposed to the eukaryotic ribosome) is limited by the only minor sequence polymorphism present in the helix 44 drug-binding pocket (14–16).

Since the discovery of streptomycin in the 1940s, numerous aminoglycosides have been isolated, and new derivatives have been synthesized. A major drawback to the clinical use of aminoglycosides has been their ototoxicity, i.e., their ability to cause irreversible hearing damage, affecting ~20% of patients in brief courses of treatment (17). This ototoxicity is linked to the destruction of the sensory cells of the inner ear and consistently has been associated with both natural and semisynthetic aminoglycosides (18). Aminoglycoside ototoxicity occurs both in a sporadic dose-dependent manner in the general patient population and in an aggravated form in genetically susceptible individuals, the latter linked to mutations in mitochondrial ribosomal RNA (rRNA), in particular the transition mutation A1555G in the A-site of the mitoribosomal small subunit (19). Despite their toxicity, aminoglycosides are still among the most commonly used antibiotics worldwide because of their high efficacy, lack of drug-related allergy, and low cost (2).

The mechanisms involved in aminoglycoside ototoxicity have been a matter of debate (17, 20–24), but compelling evidence now suggests a causal involvement of reactive oxygen species (ROS) (25, 26). The origin of ROS generation remains unresolved, however, and both nonenzymatic and enzymatic mechanisms have been suggested (27). Recent studies imply mitochondrial protein synthesis as a key element in aminoglycoside ototoxicity, because experimental evidence has been presented for both aminoglycoside-induced dysfunction of the mitochondrial ribosome, in particular drug-mediated misreading, and A1555G-linked mitochondrial hypersusceptibility to aminoglycosides (28, 29). Defective mitochondrial function reportedly elicits the formation of ROS (30, 31), and hence the antimitoribosomal activity of aminoglycosides may provoke ROS generation and/or impaired resistance to oxidative stress. Therefore the hypothesis can be put forward that aminoglycoside ototoxicity is mechanism of action related and is intimately associated with the compound's antimitoribosomal activity. This hypothesis can be tested, provided that the antibacterial activity of aminoglycosides can be separated from the compounds' activity toward the eukaryotic ribosome. We report here that apramycin, a structurally unique aminoglycoside, which is effective against a wide range of Gram-positive and Gram-negative bacteria (32–34) and which has been used in veterinary medicine but not for treatment of human infectious diseases, shows a dissociation of its bacterial and mitochondrial antiribosomal activities, giving it a low ototoxic potential. This observation provides proof of concept that drug-induced malfunction of mitochondrial ribosome is key to aminoglycoside-induced ototoxicity and provides the basis for the rational design of improved antibiotics.

Author contributions: A.V., V.R., J.S., and E.C.B. designed research; T.M., C.L.N., K.L., S.-H.S., R.A., D.S., M.M., S.D., J.X., S.R.D., and D.P.-F. performed research; T.M., C.L.N., K.L., S.-H.S., R.A., D.S., A.V., V.R., J.S., and E.C.B. analyzed data; and T.M., V.R., J.S., and E.C.B. wrote the paper.

The authors declare no conflict of interest.

*This Direct Submission article had a prearranged editor.

Data deposition: The atomic coordinates and structure factors reported in this paper have been deposited with the Protein Data Bank (PDB), www.pdb.org (PDB code 4AQY).

[1]T.M., C.L.N., K.L., S.-H.S., R.A., and D.S. contributed equally to this work.

[2]Present address: Institute of Systems Biology, Universiti Kebangsaan Malaysia, 43600 UKM, Bangi, Selangor, Malaysia.

[3]Present address: Department of Pathology and Laboratory Medicine, Medical University of South Carolina, Charleston, SC 29414.

[4]Present address: Department of Otolaryngology-Head and Neck Surgery, Beijing Tongren Hospital, Capital Medical University, Beijing 100730, China.

[5]To whom correspondence should be addressed. E-mail: boettger@imm.uzh.ch.

This article contains supporting information online at www.pnas.org/lookup/suppl/doi:10.1073/pnas.1204073109/-/DCSupplemental.

MEDICAL SCIENCES

Downloaded by guest on November 29, 2021

Results

Ribosomal Specificity of Aminoglycoside Antibiotics. To study drug specificity, we used cell-free translation assays on a range of genetically engineered hybrid ribosomes (Fig. S1). In the hybrid ribosomes a central 34-nucleotide part of the bacterial 16S rRNA helix 44 is replaced with various homologs resulting in rRNA-decoding A sites corresponding to those in human cytosolic and mitochondrial (wild-type and A1555G-mutant) ribosomes (except when it is referred to as mtDNA position 1555, the *Escherichia coli* rRNA numbering is used throughout the paper). These hybrid ribosomes have been used previously to study the ribosomal specificity of aminoglycoside antibiotics (29, 35). Dose–response curves of aminoglycoside-induced inhibition of luciferase synthesis were analyzed to define the IC_{50} values of individual aminoglycosides (Table 1). As comparators we chose the injectable 4,6-disubstituted 2-deoxystreptamines used for treatment of systemic infections in clinical medicine, i.e., gentamicin, tobramycin, and kanamycin (for chemical structures see Fig. S2*A*); the 4,5-disubstituted 2-deoxystreptamine neomycin was included because it is particularly active against mitohybrid ribosomes (29). Apramycin and the 4,6-disubstituted aminoglycosides are similarly active toward bacterial ribosomes (IC_{50} 0.02–0.08 μM) and show comparable activity for cytosolic hybrid ribosomes (IC_{50} 40.4–91.2 μM). In contrast, apramycin affects mitohybrid ribosomes significantly less than do gentamicin, tobramycin, and kanamycin. Although this difference is observed with mitohybrid ribosomes carrying the wild-type mitochondrial A site (IC_{50} for apramycin 115.6 μM versus 11.1–32.6 μM for the 4,6-disubstituted aminoglycosides), this 4- to 10-fold difference becomes 50-fold with mitohybrid ribosomes carrying the A1555G-mutant mitochondrial A site (IC_{50} for apramycin 47.5 μM versus 0.69–1.12 μM for the 4,6-disubstituted aminoglycosides).

We corroborated the findings obtained in the bacterial hybrid ribosomes by investigating native eukaryotic ribosomal particles. Rabbit reticulocyte ribosomes were used as source of eukaryotic cytosolic ribosomes and showed a drug-susceptibility pattern similar to that of the cytosolic hybrids (Table 2). Drug susceptibility of the mitoribosome was studied in an in vitro mitochondrial protein synthesis assay using *in organello* translation. As with the bacterial mitohybrid ribosomes, apramycin was significantly less active than available aminoglycosides in inhibiting mammalian mitochondrial protein translation (Fig. 1).

Structural Analysis of Apramycin–Ribosome Interaction. Crystals of the *Thermus thermophilus* 30S subunit were prepared as described previously (36). Crystals were soaked with apramycin and analyzed by X-ray diffraction. Diffraction data to 3.5-Å resolution were used to solve the structure (Fig. S2 *B* and *C*). The hydrogen-bonding pattern and position of the apramycin 2-deoxystreptamine moiety (ring I) are similar to those of the 2-deoxystreptamine ring of 4,6-disubstituted aminoglycosides, with hydrogen bonds between apramycin N3 and N7 of G1494 and apramycin N1 and O4 of U1495. The bicyclic ring II of apramycin lies above and parallel to the guanine base of the C1409-G1491 base pair, with the ring oxygen and the 6′ hydroxyl forming hydrogen bonds to N6 and N1 of A1408, resulting in a pseudo base pair interaction with A1408. Ring III mainly points out into the solvent. However, its O6 is 3.5 Å from the N3 of A1491, and its 2-OH is 3.7 Å away from the no-bridging phosphate oxygen of A1493.

Table 1. Aminoglycoside interaction with drug-binding pockets: Bacterial wild-type and hybrid ribosomes

	Bacterial wild-type and hybrid ribosomes: A site rRNA*			
Aminoglycoside	Bacterial	Mitochondrial hybrid	Mitochondrial A1555G hybrid	Cytosolic hybrid
Apramycin	0.08 ± 0.02	115.6 ± 27.8	47.5 ± 10.7	89.4 ± 21.2
Gentamicin	0.02 ± 0.01	11.1 ± 1.6	0.69 ± 0.12	40.4 ± 10.4
Tobramycin	0.03 ± 0.01	32.6 ± 2.1	1.07 ± 0.19	58.5 ± 11.8
Kanamycin	0.04 ± 0.02	31.1 ± 14.3	1.12 ± 0.16	91.2 ± 12.3
Neomycin	0.02 ± 0.01	2.64 ± 0.58	0.35 ± 0.08	37.9 ± 11.2

*Aminoglycoside induced inhibition of protein synthesis (IC_{50} μM). IC_{50} values represent the drug concentrations in micromolars required to inhibit in vitro synthesis of functional firefly luciferase to 50% (mean and SD of experiments performed in triplicate).

Table 2. Aminoglycoside interaction with drug-binding pockets: rabbit ribosomes

Aminoglycoside	Rabbit reticulocyte extract*
Apramycin	48.3 ± 10.2
Tobramycin	81.1 ± 18.2
Kanamycin	50.5 ± 7.8
Neomycin	35.9 ± 10.1

*Aminoglycoside induced inhibition of protein synthesis (IC_{50} μM). IC_{50} values represent the drug concentrations in micromolars required to inhibit in vitro synthesis of functional firefly luciferase to 50% (mean and SD of experiments performed in triplicate).

Mutagenesis Studies. We used the X-ray crystallography data to rationalize the structural basis of the differences in ribosomal specificity (Tables 1 and 2) between apramycin and the other aminoglycosides that bind in the decoding center. The bicyclic ring II of apramycin stacks less well onto G1491 than the more flexible monocyclic ring I in 4,6-disubstituted 2-deoxystreptamines, and the 6′ substituent of apramycin, interacting by hydrogen bonding with N1 of A1408, is an axial hydroxyl as opposed to an equatorial amino group in the disubstituted 2-deoxystreptamines. These features should restrain apramycin's flexibility to accommodate the phylogenetic sequence polymorphism present in h44. In particular, its binding should be highly sensitive to mutations of nucleotides 1491 and 1408. For example, a 1408 A→G mutation would replace the hydrogen bond between the ring oxygen of the bicyclic ring II and N6 of adenine by a repulsive interaction with the O6 of guanine. We tested the effects of mutations in A1408 and G1491 by studying drug susceptibility of recombinant microorganisms with the A-site modified by site-directed mutagenesis (Table 3). An A1408G mutation conferred high-level resistance, as did any mutational alteration of residue G1491. This pattern of ribosomal drug susceptibility was corroborated in cell-free translation assays (Table 4).

Aminoglycoside-Induced Misreading. Next, drug-induced misreading in mitohybrid ribosomes was assessed in a dual-luciferase (37) gain-of-function assay. Mutation at amino acid 245 (wild-type CAC histidine) in the active site of firefly luciferase results in loss of enzymatic activity, and enzymatic function can be restored by misreading. Aminoglycoside-induced misreading is codon-restricted, with the near-cognate CGC codon being used as test codon and the noncognate AGA codon as negative control (38, 39). Wild-type renilla luciferase activity serves as internal standard to monitor translation activity. In contrast to the comparator aminoglycosides, apramycin shows very little, if any, misreading on both wild-type mitohybrid and A1555G-mutant mitohybrid ribosomes (Fig. 2 *A* and *B*).

Lack of misreading induction by apramycin also is observed in bacterial ribosomes (Fig. 2 *C* and *D* and Fig. S3). The data on the structure and function of apramycin–ribosome interaction invite the question of how apramycin avoids misreading induction. Compared with the 30S apramycin crystal structure, which was fitted in the presence of a cognate tRNA/anticodon stem loop positioned in the A-site, a bacterial A-site oligonucleotide apramycin complex suggests a hydrogen bond interaction between ring III 2" OH and the ribose moiety of A1492 (40). This interaction possibly could interfere with the switch of residue A1492 to adopt a fully flipped-out conformation as is associated with aminoglycoside-induced misreading (10). This hypothesis, based on the available bacterial structures, predicts that, in

Downloaded by guest on November 29, 2021

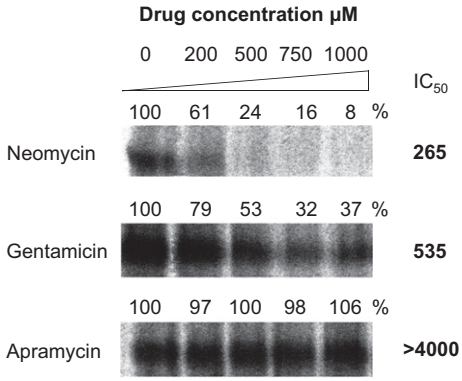

Fig. 1. Mitochondrial *in organello* translation: aminoglycoside effects on mitochondrial protein synthesis. Isolated mitochondria were incubated with various concentrations of aminoglycosides as indicated. Proteins were resolved by SDS/PAGE, and COX1 protein levels were quantified by densitometry. Images of the relevant part of the SDS gel used for quantitation are shown. Quantitation is given in percent. IC_{50} values indicate the drug concentration in micromolars required to inhibit COX1 synthesis by 50%.

contrast to apramycin, aprosamine—which is identical to apramycin except that it lacks the terminal ring III (for chemical structure of aprosamine, see Fig. 2*A*)—readily should induce misreading on bacterial ribosomes. To test the hypothesis, we synthesized aprosamine following published procedures and assessed misreading induction on bacterial ribosomes. In contrast to apramycin, aprosamine readily induced misreading (Fig. 2 and Fig. S3).

In Vitro and in Vivo Toxicity Studies. In organ cultures of the early postnatal mouse, treatment with gentamicin caused the typical ototoxic pattern of hair cell loss, namely a preferential loss of outer hair cells in a base-to-apex gradient that is characteristic of aminoglycoside damage to the cochlea in both human and experimental animals. The dose–response curve shows that 50% of all outer hair cells and 100% of hair cells in the base of the cochlea were destroyed at 0.2 mM gentamicin, and complete elimination of outer hair cells was observed at 0.5 mM. In keeping with the established pattern of cochlear damage, inner hair cells were partly spared. In contrast, apramycin at a dose of 0.2 mM does not affect cells adversely even in the base of the cochlea, the most vulnerable region. At 2 mM, apramycin begins to affect basal hair cells but does not cause a significant overall loss of hair cells (Fig. 3 *A* and *B*).

3-Nitrotyrosine, indicative of peroxynitrite formation, was assayed as a marker for oxidative stress. Nitrotyrosine was absent from control incubations (Fig. 3 *C a*) but after 16 h was observed readily in the basal regions of explants damaged by 0.2 mM gentamicin (Fig. 3 *C b*). Treatment with 2 mM apramycin for 16 h resulted in little nitrotyrosine formation (Fig. 3 *C c*). There was no immunoreactivity to nitrotyrosine with 0.2 mM apramycin or in the undamaged regions of the explants treated with 2 mM apramycin.

Table 3. Aminoglycoside interaction with mutant drug-binding pockets: A site mutagenesis and aminoglycoside susceptibility assessed in MIC assays (mg/L)

A site	Apramycin	Gentamicin	Tobramycin	Kanamycin
Wild type	1–2	1	1	2–4
A1408G	>1,024	>1,024	1,024	>1,024
G1491A	256	2	2	8
G1491U	>1,024	32	64	64
G1491C	>1,024	16	16	32

Table 4. Aminoglycoside interaction with mutant drug-binding pockets: Mutant A sites and drug susceptibility tested in cell-free translation assays (luciferase synthesis, IC_{50})

A site	Apramycin	Gentamicin	Tobramycin	Kanamycin
Wild type	0.08 ± 0.02	0.02 ± 0.01	0.03 ± 0.01	0.04 ± 0.02
A1408G	257.8 ± 72.9	121.7 ± 63.6	113.7 ± 47.3	103.1 ± 28.3
G1491A	9.96 ± 2.40	0.16 ± 0.02	0.25 ± 0.01	0.18 ± 0.04
G1491C	61.6 ± 12.4	1.35 ± 0.02	3.04 ± 0.03	1.61 ± 0.21

IC_{50} values represent the drug concentrations in micromolars required to inhibit in vitro synthesis of functional firefly luciferase to 50% (mean and SD of experiments performed in triplicate).

The differential toxicity of gentamicin and apramycin was assessed further in vivo by measuring auditory brain response (ABR) at 12 kHz and loss of hair cells in the guinea pig. Gentamicin ototoxicity rises very steeply from essentially no effect on auditory thresholds at 120 mg/kg body weight to complete deafness at 160 mg/kg (Fig. 3*D*). In contrast, apramycin ototoxicity progresses more gradually, and cochlear function was partly retained even at a concentration of 430 mg apramycin/kg body weight. Loss of hair cells seen in cochlear surface preparations was consistent with the functional results obtained from the ABR measurements. Treatment with 140 mg gentamicin/kg body weight resulted in a base-to-apex gradient of hair cell loss with a complete destruction of hair cells in the basal half of the cochlea. After treatment with 217 mg apramycin/kg body weight, only scattered hair cell loss was observed (Fig. S4).

To address whether apramycin alleviation from aminoglycoside ototoxicity in vivo reflects differences in accessibility of eukaryotic cytosolic protein synthesis to aminoglycoside action, we studied drug susceptibility of cytosolic protein synthesis at the whole-cell level using HEK293 cells. No significant difference was found between apramycin and tobramycin (Fig. S5 *A* and *B*), effectively ruling out the possibility that apramycin alleviation from ototoxicity relates to differences in drug uptake or differences in accessibility of cytosolic protein synthesis to aminoglycoside compounds.

Antibacterial Activity. We assessed the antimicrobial activity of apramycin by determining minimal inhibitory concentration (MIC) values of recombinant *E. coli* carrying defined aminoglycoside-resistance determinants (41) and by testing various clinical isolates. Apramycin shows good activity against recombinant *E. coli* with defined resistance determinants and against aminoglycoside-resistant clinical isolates of *E. coli*, *Pseudomonas aeruginosa,* and *Staphylococcus aureus*, including methicillin-resistant *S. aureus* (MRSA) (Tables S1 and S2). Of note, the bactericidal potency of aminoglycosides does not require bacterioribosomal misreading, because the bactericidal activity of the nonmisreader apramycin was similar to that of the misreader gentamicin (Fig. S5*C*). Apramycin also shows good antimycobacterial activity against various clinical isolates including *Mycobacterium tuberculosis*, *Mycobacterium abscessus*, *Mycobacterium massiliense*, and *Mycobacterium bolletii* (Tables S3–S5). Apramycin's in vitro activity against *M. tuberculosis* is similar to that of amikacin, an established second-line antituberculous agent (42).

Discussion

Apramycin is structurally unique among the aminoglycosides in that it contains a bicyclic sugar moiety and a monosubstituted 2-deoxystreptamine ring (32, 34). The unusual structure of apramycin precludes its inactivation by many of the known aminoglycoside-modifying enzymes (33). As a result, apramycin shows good activity against a range of clinical aminoglycoside-resistant pathogens. More recently, and in comparison with all human-use aminoglycosides, apramycin has been found to be the only aminoglycoside active against carbapenem-resistant enterobacterial isolates carrying ArmA and RmtC 16S rRNA methylases, such as the emerging NDM-1 resistance plasmid (43). Of note, apramycin exhibits high antimycobacterial activity, including

Downloaded by guest on November 29, 2021

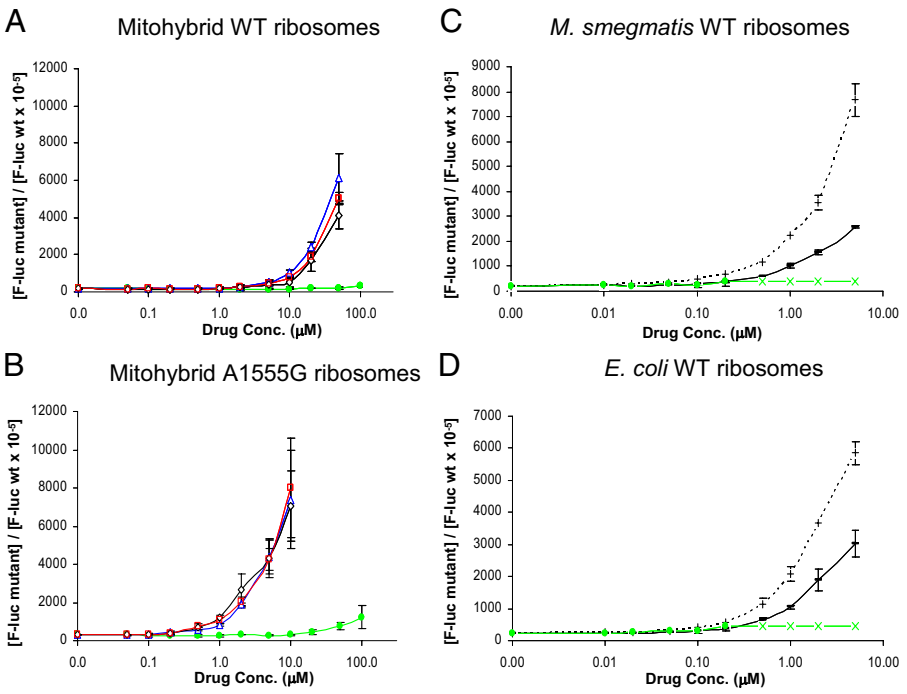

Fig. 2. Aminoglycoside-induced misreading. Dose–response curves of aminoglycoside-induced misincorporation of amino acids using 245 near-cognate CGC-mutant firefire luciferase (F-luc) mRNA as template. Shown is luciferase activity upon translation of mutant template relative to wild-type F-luc mRNA (mean ± SD; n = 3). Mitochondrial wild-type hybrid (Mit13) ribosomes (*A*) and mitochondrial A1555G-mutant hybrid ribosomes (*B*) treated with apramycin (filled green circles), gentamicin (blue open triangles), tobramycin (open black rhombi), or kanamycin (open red squares). *Mycobacterium smegmatis* bacterial ribosomes (*C*) and *E. coli* bacterial ribosomes (*D*) treated with apramycin (filled green circles and solid green line) or aprosamine (dashes and solid black line). Neamine (crosses and dotted black line) was used as control. Green crosses indicate misreading values below background.

M. tuberculosis and rapidly growing nontuberculous mycobacteria, such as *M. abscessus*, *M. massiliense*, and *M. bolletii*. The latter three are difficult-to-treat, obnoxious lung pathogens in patients with cystic fibrosis or bronchiectasis, and apramycin's excellent activity, more potent than that of any other aminoglycoside including the gold standard amikacin, makes it particularly promising. Apramycin was also tested for its ability to inhibit the growth of multidrug-resistant (MDR) clinical strains of *M. tuberculosis*. Apramycin susceptibility of strains exhibiting the MDR phenotype was indistinguishable from that determined for non-MDR clinical isolates (Tables S3 and S4). Combined with the compound's low ototoxic potential, this efficacy makes apramycin a drug of immediate clinical interest.

The molecular basis underlying the unique characteristic of potent antibacterial activity combined with low ototoxicity is rationalized by the ribosomal selectivity of apramycin, i.e., the compound's ability to affect prokaryotic and eukaryotic (mitochondrial, cytosolic) ribosomes differentially. Together with the clinically used 4,6-disubstituted 2-deoxystreptamines gentamicin, tobramycin, and kanamycin, apramycin shows high activity for bacterial ribosomes and comparable selectivity for eukaryotic cytosolic ribosomes. In contrast to the other drugs, however, apramycin affects the mitochondrial ribosome considerably less. Most significantly, apramycin does not show much of a preferential activity for the A1555G mutant compared with the wild-type mitochondrial hybrid ribosomes, as is typical for 4,6- and 4,5-aminoglycosides (28, 29). Similar to gentamicin, tobramycin, and kanamycin, apramycin shows little activity toward bacterial A1408G mutants. In contrast to the former aminoglycosides and unique to apramycin is the sensitivity to any alteration of residue G1491. Because aminoglycoside selectivity rests upon single-nucleotide differences in the A-site (G1408, A1491 in eukaryotic cytosolic ribosomes; C1491 in eukaryotic mitoribosomes), these findings provide an adequate explanation for the increased selectivity of apramycin compared with the disubstituted 2-deoxystreptamine aminoglycosides.

Aminoglycoside-induced mitochondrial mistranslation has been suggested as a key element in aminoglycoside ototoxicity (28, 29). In contrast to the 4,6-disubstituted 2-deoxystreptamines, apramycin does not show significant misreading on mitochondrial wild-type and A1555G-mutant hybrid ribosomes. In the absence of established procedures for crystallization of higher eukaryotic mitoribosomes, we infer the structural basis for the lack of misreading from the details offered by crystals of the bacterial ribosome in complex with apramycin. The unique structure of the apramycin-h44 complex, with ring III positioned in the minor groove of the 1409–1491 base pair, suggests a possible hypothesis for the apramycin's low capacity for inducing misreading, as compared with the disubstituted 2-deoxystreptamines. For comparison, an overlay of the structures of apramycin and that of the disubstituted 2-deoxystreptamine paromomycin is shown in Fig. S2*D*. Ring III of apramycin has an orientation orthogonal to the plane of the 1409–1491 base pair, possibly allowing the formation of direct hydrogen bonds between the highly flexible A1492 and ring III. Indeed, such a hydrogen bond interaction between ring III 2" OH and the ribose moiety of A1492 is suggested by the bacterial oligonucleotide structure (40). In contrast to the disubstituted 2-deoxystreptamines, which displace A1492/A1493 directly into a position where they make contact with the minor groove of the codon-anticodon helix and thereby induce accommodation of near-cognate tRNA (i.e., misreading), apramycin might be able to stabilize a flipped-out A1492 partially, in an intermediate position. As a result, apramycin does not induce misreading. We tested this hypothesis experimentally by synthesis of aprosamine, which lacks the terminal sugar (ring III) of apramycin. The binding mode of 4,5-aminoglycosides, 4,6-aminoglycosides, and the 4-monosubstituted apramycin is highly conserved. Apramycin's 2-deoxystreptamine moiety interacts with h44 in a manner nearly identical to that of the 2-deoxystreptamine moiety of 4,5- and 4,6-aminoglycosides, and apramycin's bicyclic ring II shows an orientation similar to that of ring I of the 4,5- and 4,6-aminoglycosides. Taken together, these observations allow the conclusion that aprosamine will bind in a manner similar to apramycin. However, in contrast to apramycin, aprosamine readily induced misreading on bacterial ribosomes, as predicted by our hypothesis that ring III interferes with the switch of residue A1492 to adopt a flipped-out conformation—a key structural alteration associated with aminoglycoside-induced misreading (10).

We used cultures of murine organ of Corti explants (44, 45) and in vivo studies in the guinea pig (46) to compare the ototoxicity of apramycin with that of gentamicin, a well-characterized and commonly used aminoglycoside with known ototoxicity to animals and humans. The lesser hair cell toxicity of apramycin observed in organ Corti explants is borne clearly out in the

Downloaded by guest on November 29, 2021

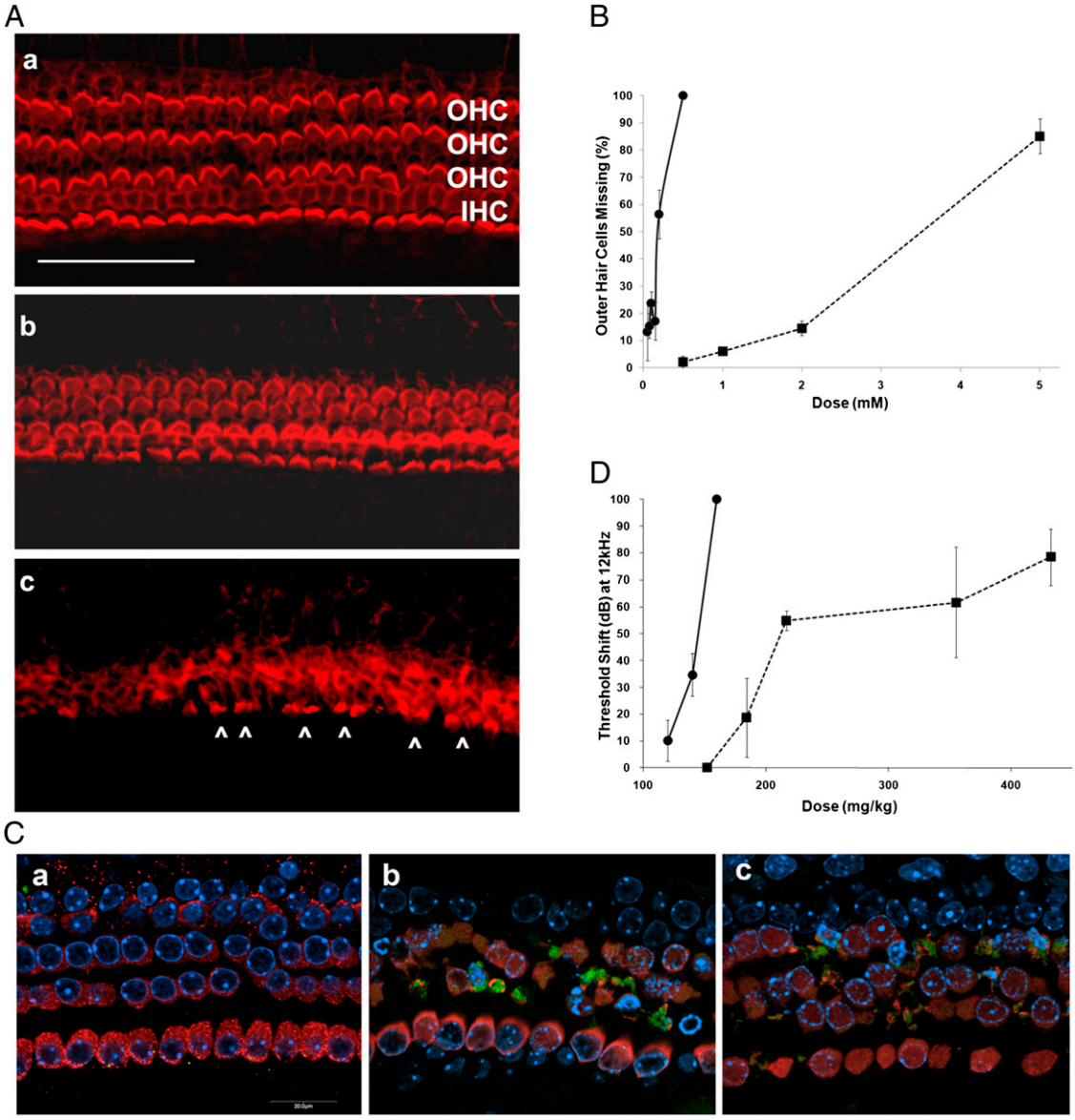

Fig. 3. Loss of hair cells in cochlear explants and loss of auditory function in vivo. (*A*) Hair cells in mouse organ of Corti explants were stained for actin with rhodamine-phalloidin. (*a*) Control. (*b*) Treatment with 0.2 mM apramycin. (*c*) Treatment with 0.2 mM gentamicin. Panels *a* and *b* show normal morphology with one row of inner hair cells (IHC) and three rows of outer hair cells (OHC). (OHC row 1 is adjacent to IHC.) In *c* loss of OHC is essentially complete, but some IHC (arrowheads) remain. Sections are from the upper basal turn of the cochlea. (Scale bar: 50 μm.) (*B*) Hair cell loss was quantified along the entire length of cochlear explants and plotted against drug concentration of gentamicin (circles and solid line) and apramycin (squares and dotted line). Data represent means ± SEM, n = 3–12 per point. (*C*) Explants of the organ of Corti were stained with antibody to 3-nitrotyrosine (green); blue staining (Hoechst 33342) shows nuclei, and red staining is myosin VIIa antibody outlining hair cells. (*a*) Control. (*b*) Treatment with 0.2 mM gentamicin. (*c*) Treatment with 2 mM apramycin. (*D*) Effect of chronic aminoglycoside treatment (gentamicin, circles and solid line; apramycin, squares and dotted line) in vivo on ABR. Threshold shift is the difference in auditory threshold before and 3 wk after treatment. Data represent means ± SEM, n = 3–11 per point (except for 160 mg gentamicin, in which only one animal survived). The threshold shift was determined in dB, corresponding to a logarithmic scale (i.e., a 10-dB difference indicates a 1 $\log_{10}$ difference in energy).

pathology and pathophysiology caused in vivo. In contrast to the effects of gentamicin, hearing loss induced by apramycin developed more gradually and only at higher drug concentrations. Consistent with the functional results obtained from ABR measurements, the in vivo treatment with apramycin resulted in little hair cell loss as revealed in a dose-by-dose comparison with gentamicin. Guinea pigs treated with gentamicin also showed signs of general toxicity. At a dose of 140 mg gentamicin/kg body weight all eight animals had significant lower weight gain than did saline-treated controls, and at a dose of 160 mg/kg body weight, two of three animals died early during the experiments. In contrast, all animals treated with apramycin remained healthy during the complete course of the experiment, and even at a dose of 430 mg/kg body weight no drug-related death was observed. Renal necropsy and analysis of blood urea nitrogen and creatinine likewise did not reveal any nephrotoxic side effects of apramycin. It also should be noted that the concentrations of drugs used in animal models exceed those used in clinical medicine by an order of magnitude so as to obtain relatively high and reliable ABR threshold shifts. The clinical incidence of gentamicin ototoxicity ranges from 10 to >20% in treatment of acute infections (17), and the much lesser toxicity of apramycin should provide a significant safety margin and considerably fewer side effects.

Downloaded by guest on November 29, 2021

For a mechanistic exploration of ototoxicity, the emergence of the ROS marker nitrotyrosine in the organotypic cultures is revealing. In accordance with its lesser toxicity, apramycin does not elicit ROS at low drug concentrations. However, for both gentamicin and apramycin, the appearance of nitrotyrosine becomes evident at antibiotic levels that begin to cause loss of hair cells. This correlation with ototoxicity, rather than with drug concentration, supports the notion that generation of ROS is an integral part of the mechanisms that lead to cell death. Taken together with the data on antimitoribosomal activities, an interplay of mitochondrial mistranslation and ROS formation resulting in cell death becomes a logical postulate for a mechanism of ototoxicity. In contrast, the low ototoxicity associated with apramycin is difficult to reconcile with the alternate suggestion that aminoglycoside ototoxicity is related to NMDA receptor activation (22), because apramycin shows NMDA receptor activation similar to that of the highly ototoxic neomycin (47).

In conclusion, our structural, biochemical, and toxicology studies have revealed properties of apramycin that can be exploited in the treatment of human infectious diseases, including treatment of tuberculosis and MDR tuberculosis. Our data identify apramycin as a unique aminoglycoside with a dissociation of antibacterial and antimitoribosomal activity. We demonstrate proof of concept and provide explanations for this surprising observation. Following decades of trial-and-error synthesis in attempts to develop less toxic aminoglycoside derivatives, our data may provide the rationale for hypothesis-driven modification of aminoglycosides by chemical synthesis to improve further this important class of antibacterials.

Methods

Methods for construction of mutant strains, isolation and purification of ribosomes, luciferase translation assays, mitochondrial *in organello* translation, aminoglycoside-induced inhibition of protein synthesis, MIC determinations, crystal structure analysis, and assay of ototoxicity are included in *SI Methods*. Plasmids used for genetic manipulations and recombinant strains generated are summarized in Tables S6 and S7. Sources of bacterial strains and antibiotics are given in *SI Methods*. Crystallographic data and refinement are provided in Table S8.

ACKNOWLEDGMENTS. We thank Tanja Janusic, Sven Hobbie, Claudia Ritter, Akshay Subramanian, Sarath Kalapala, and Kimberly Wearne for help and expert technical assistance, Ann Kelley for preparing the 30 crystals, the members of the E.C.B. laboratory for stimulating discussions during the entire work, and Susanna Salas and Franziska Mitterecker for help with the manuscript. We thank Patrice Courvalin, Institut Pasteur, for providing recombinant *E. coli* strains. This study was supported in part by grants from the University of Zurich and the European Community (PAR, FP-7 HEALTH-2009-241476) (to E.C.B.) and by Grant DC-003685 from the National Institute on Deafness and other Communication Disorders, National Institutes of Health (to J.S.). V.R. was supported by the Medical Research Council UK and the Wellcome Trust.

1. Gale EF, Cundliffe E, Reynolds PE, Richmond MH, Waring MJ (1981) *The Molecular Basis of Antibiotic Action* (London, John Wiley and Sons) 2nd Ed.
2. Chambers HF (1996) Chemotherapy of microbial diseases. *Goodman and Gilman's The Pharmaceutical Basis of Therapeutics* (McGraw-Hill, New York), 10th Ed.
3. Moazed D, Noller HF (1987) Interaction of antibiotics with functional sites in 16S ribosomal RNA. *Nature* 327:389–394.
4. Davies JL, Gorini L, Davis BD (1965) Misreading of RNA codewords induced by aminoglycoside antibiotics. *Mol Pharmacol* 1:93–106.
5. Benveniste R, Davies J (1973) Structure-activity relationships among the aminoglycoside antibiotics: Role of hydroxyl and amino groups. *Antimicrob Agents Chemother* 4:402–409.
6. Cabañas MJ, Vázquez D, Modolell J (1978) Inhibition of ribosomal translocation by aminoglycoside antibiotics. *Biochem Biophys Res Commun* 83:991–997.
7. Pape T, Wintermeyer W, Rodnina MV (2000) Conformational switch in the decoding region of 16S rRNA during aminoacyl-tRNA selection on the ribosome. *Nat Struct Biol* 7:104–107.
8. Peske F, Savelsbergh A, Katunin VI, Rodnina MV, Wintermeyer W (2004) Conformational changes of the small ribosomal subunit during elongation factor G-dependent tRNA-mRNA translocation. *J Mol Biol* 343:1183–1194.
9. Feldman MB, Terry DS, Altman RB, Blanchard SC (2010) Aminoglycoside activity observed on single pre-translocation ribosome complexes. *Nat Chem Biol* 6:54–62.
10. Carter AP, et al. (2000) Functional insights from the structure of the 30S ribosomal subunit and its interactions with antibiotics. *Nature* 407:340–348.
11. Vicens Q, Westhof E (2001) Crystal structure of paromomycin docked into the eubacterial ribosomal decoding A site. *Structure* 9:647–658.
12. François B, et al. (2005) Crystal structures of complexes between aminoglycosides and decoding A site oligonucleotides: Role of the number of rings and positive charges in the specific binding leading to miscoding. *Nucleic Acids Res* 33:5677–5690.
13. Hobbie SN, Pfister P, Brüll C, Westhof E, Böttger EC (2005) Analysis of the contribution of individual substituents in 4,6-aminoglycoside-ribosome interaction. *Antimicrob Agents Chemother* 49:5112–5118.
14. Böttger EC, Springer B, Prammananan T, Kidan Y, Sander P (2001) Structural basis for selectivity and toxicity of ribosomal antibiotics. *EMBO Rep* 2:318–323.
15. Böttger EC (2007) Antimicrobial agents targeting the ribosome: The issue of selectivity and toxicity - lessons to be learned. *Cell Mol Life Sci* 64:791–795.
16. Fan-Minogue H, Bedwell DM (2008) Eukaryotic ribosomal RNA determinants of aminoglycoside resistance and their role in translational fidelity. *RNA* 14:148–157.
17. Forge A, Schacht J (2000) Aminoglycoside antibiotics. *Audiol Neurootol* 5:3–22.
18. Davies J (2007) In the beginning there was streptomycin. *Aminoglycoside Antibiotics* (John Wiley & Sons, Hoboken, NJ).
19. Prezant TR, et al. (1993) Mitochondrial ribosomal RNA mutation associated with both antibiotic-induced and non-syndromic deafness. *Nat Genet* 4:289–294.
20. Xie J, Talaska AE, Schacht J (2011) New developments in aminoglycoside therapy and ototoxicity. *Hear Res* 281:28–37.
21. Leitner MG, Halaszovich CR, Oliver D (2011) Aminoglycosides inhibit KCNQ4 channels in cochlear outer hair cells via depletion of phosphatidylinositol(4,5)bisphosphate. *Mol Pharmacol* 79:51–60.
22. Basile AS, et al. (1996) N-methyl-D-aspartate antagonists limit aminoglycoside antibiotic-induced hearing loss. *Nat Med* 2:1338–1343.
23. Sha SH, Schacht J (1998) Are aminoglycoside antibiotics excitotoxic? *Neuroreport* 9: 3893–3895.
24. Kalinec GM, et al. (2005) Pivotal role of Harakiri in the induction and prevention of gentamicin-induced hearing loss. *Proc Natl Acad Sci USA* 102:16019–16024.
25. Sha SH, Schacht J (1999) Stimulation of free radical formation by aminoglycoside antibiotics. *Hear Res* 128:112–118.
26. Talaska AE, Schacht J (2007) Adverse effects of aminoglycoside therapy. *Aminoglycoside Antibiotics* (John Wiley & Sons, Hoboken, NJ).
27. Jiang H, Sha SH, Schacht J (2006) Rac/Rho pathway regulates actin depolymerization induced by aminoglycoside antibiotics. *J Neurosci Res* 83:1544–1551.
28. Hobbie SN, et al. (2008) Mitochondrial deafness alleles confer misreading of the genetic code. *Proc Natl Acad Sci USA* 105:3244–3249.
29. Hobbie SN, et al. (2008) Genetic analysis of interactions with eukaryotic rRNA identify the mitoribosome as target in aminoglycoside ototoxicity. *Proc Natl Acad Sci USA* 105: 20888–20893.
30. Pieczenik SR, Neustadt J (2007) Mitochondrial dysfunction and molecular pathways of disease. *Exp Mol Pathol* 83:84–92.
31. Wu SB, Ma YS, Wu YT, Chen YC, Wei YH (2010) Mitochondrial DNA mutation-elicited oxidative stress, oxidative damage, and altered gene expression in cultured cells of patients with MERRF syndrome. *Mol Neurobiol* 41:256–266.
32. O'Connor S, Lam LK, Jones ND, Chaney MO (1976) Apramycin, a unique aminocyclitol antibiotic. *J Org Chem* 41:2087–2092.
33. Ryden R, Moore BJ (1977) The in vitro activity of apramycin, a new aminocyclitol antibiotic. *J Antimicrob Chemother* 3:609–613.
34. Perzynski S, Cannon M, Cundliffe E, Chahwala SB, Davies J (1979) Effects of apramycin, a novel aminoglycoside antibiotic on bacterial protein synthesis. *Eur J Biochem* 99:623–628.
35. Hobbie SN, et al. (2007) Engineering the rRNA decoding site of eukaryotic cytosolic ribosomes in bacteria. *Nucleic Acids Res* 35:6086–6093.
36. Wimberly BT, et al. (2000) Structure of the 30S ribosomal subunit. *Nature* 407: 327–339.
37. Grentzmann GJ, Ingram JA, Kelly PJ, Gesteland RF, Atkins JF (1998) A dual-luciferase reporter system for studying recoding signals. *RNA* 4:479–486.
38. Salas-Marco J, Bedwell DM (2005) Discrimination between defects in elongation fidelity and termination efficiency provides mechanistic insights into translational readthrough. *J Mol Biol* 348:801–815.
39. Kramer EB, Vallabhaneni H, Mayer LM, Farabaugh PJ (2010) A comprehensive analysis of translational missense errors in the yeast *Saccharomyces cerevisiae*. *RNA* 16: 1797–1808.
40. Han Q, et al. (2005) Molecular recognition by glycoside pseudo base pairs and triples in an apramycin-RNA complex. *Angew Chem Int Ed Engl* 44:2694–2700.
41. Wright GD, Berghuis AM, Mobashery S (1998) Aminoglycoside antibiotics. Structures, functions, and resistance. *Adv Exp Med Biol* 456:27–69.
42. Mukherjee JS, et al. (2004) Programmes and principles in treatment of multidrug-resistant tuberculosis. *Lancet* 363:474–481.
43. Livermore DM, et al. (2011) Activity of aminoglycosides, including ACHN-490, against carbapenem-resistant Enterobacteriaceae isolates. *J Antimicrob Chemother* 66:48–53.
44. Zheng JL, Gao WQ (1996) Differential damage to auditory neurons and hair cells by ototoxins and neuroprotection by specific neurotrophins in rat cochlear organotypic cultures. *Eur J Neurosci* 8:1897–1905.
45. Chen F-Q, Schacht J, Sha SH (2009) Aminoglycoside-induced histone deacetylation and hair cell death in the mouse cochlea. *J Neurochem* 108:1226–1236.
46. Garetz SL, Schacht J (1996) Ototoxicity: Of mice and men. *Clinical Aspects of Hearing. Handbook of Auditory Research*, eds van de Water TR, Popper AN, Fay RR. (Springer, New York), Vol. 7, pp 116–154.
47. Harvey SC, Li X, Skolnick P, Kirst HA (2000) The antibacterial and NMDA receptor activating properties of aminoglycosides are dissociable. *Eur J Pharmacol* 387:1–7.

Downloaded by guest on November 29, 2021